Taebi, S., R. J. Lowe, C. B. Pattiaratchi, G. N. Ivey, G. Symonds, and R. Brinkman (2011), Nearshore circulation in a tropical fringing reef system, J. Geophys. Res., 116, C02016, doi: 10.1029/2010JC006439.

Nearshore circulation in a tropical fringing reef system

Soheila Taebi,[1,2] Ryan J. Lowe,[2,3] Charitha B. Pattiaratchi,[1,2] Greg N. Ivey,[1,2] Graham Symonds,[4] and Richard Brinkman[5]

Received 28 May 2010; revised 18 November 2010; accepted 7 December 2010; published 12 February 2011.

[1] The role of waves, tide, and wind on the circulation of a fringing reef system was investigated using data collected during a 6 week field experiment in a section of Ningaloo Reef off Western Australia. The high correlation observed between current velocities and wave height throughout the system revealed the dominant role wave breaking plays in driving the overall reef-lagoon circulation, whereas the modulation of the currents at tidal frequencies suggested that the wave-driven currents responded to tidal variations in the mean water level over the reef. The influence of the various forcing mechanisms on the current field was investigated for both high- and low-frequency bands. Wave breaking was found to be the dominant forcing mechanism for the low-frequency (subtidal) currents, with the subtidal flow pattern consisting of a cross-reef flow over the reef, alongshore flow in the lagoon, and water exiting back to the ocean through the main channel. The tides controlled the high-frequency current variability via two mechanisms: one associated with the ebb-flood cycle of the tides and the second associated with tidal modulations of the wave-driven currents. Wind-forcing and buoyancy effects were both found to be negligible in driving the circulation and flushing of the system during the observation period. Flushing time scale estimates varied from as low as 2 h to more than a day for the wide range of observed incident wave heights. The results suggest that the circulation of Ningaloo Reef will be strongly influenced by even a small mean sea level rise.

Citation: Taebi, S., R. J. Lowe, C. B. Pattiaratchi, G. N. Ivey, G. Symonds, and R. Brinkman (2011), Nearshore circulation in a tropical fringing reef system, *J. Geophys. Res.*, *116*, C02016, doi:10.1029/2010JC006439.

1. Introduction

[2] Water motion is known to control a number of key ecological and biogeochemical processes on coral reefs, such as biogeographic zonation [e.g., *Grigg*, 1998], rates of nutrient uptake by coral reef communities [e.g., *Atkinson and Falter*, 2003], and the transport and dispersal of larval coral and other reef organisms [e.g., *Kraines et al.*, 2001; *Pattiaratchi*, 1994]. In general, the circulation within coral reef systems can be driven by a number of forcing mechanisms, including surface wave breaking, tides, wind and buoyancy effects [*Monismith*, 2007]. The relative importance of each of these mechanisms depends not only on the external forcing climate present at a given site, but may also depend strongly on the particular morphology of the reef itself [*Lowe et al.*, 2009b]. For wave exposed reefs, many studies have observed that reef circulation is dominated by the effects of depth-limited wave breaking [e.g., *Monismith*, 2007]. The dynamics of these wave-driven reef flows thus have some broad similarities to the currents generated by waves in other nearshore systems, such as on beaches [e.g., *MacMahan et al.*, 2006]. On reefs, wave breaking on the reef slope (forereef) generates cross-shore gradients in the radiation stress (i.e., the excess momentum due to the presence of the waves) [*Longuet-Higgins and Stewart*, 1964]. On beaches, the cross-shore gradients in radiation stress are balanced by an offshore pressure gradient, producing well-known wave setup through the surf zone [*Bowen et al.*, 1968; *Guza and Thornton*, 1981]. But on a reef, where the depth is finite at the inner edge of the surf zone (i.e., on the reef flat), the cross-shore gradients in radiation stress also drive mean currents through the surf zone (Figure 1). Over the reef flat, the cross-shore gradients in radiation stress effectively vanish once wave dissipation ceases outside the surf zone, but continuity requires a current to match the cross-shore volume flux through the surf zone. This causes a pressure gradient to develop across the reef flat with an increase in sea level (wave setup) at the top of the reef slope, which in turn produces a pressure gradient through the surf zone opposing the flow. Therefore, on a reef the cross-reef gradient in

[1]School of Environmental Systems Engineering, University of Western Australia, Crawley, Western Australia, Australia.
[2]Oceans Institute, University of Western Australia, Crawley, Western Australia, Australia.
[3]School of Earth and Environment, University of Western Australia, Crawley, Western Australia, Australia.
[4]Marine and Atmospheric Research, CSIRO, Floreat, Western Australia, Australia.
[5]Australian Institute of Marine Science, Townsville, Queensland, Australia.

0148-0227/11/2010JC006439

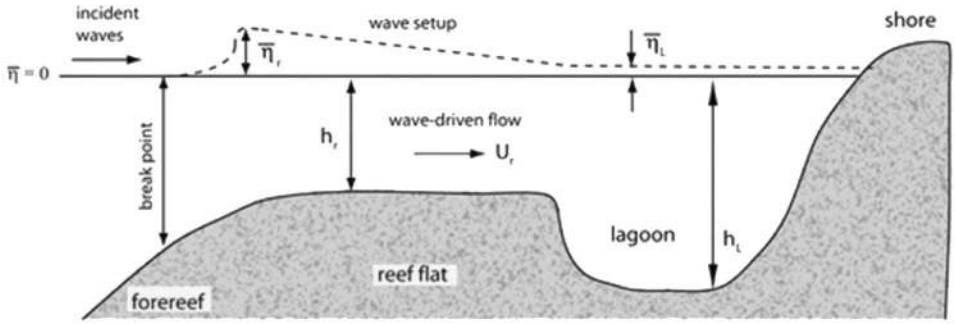

Figure 1. An idealized cross section of a fringing coral reef system showing the dominant reef morphological features, including a sloping forereef, a shallow reef flat, a deeper lagoon, and the shore (adapted from *Lowe et al.* [2009b]). Spatial differences in wave setup $\overline{\eta}$ between the reef ($\overline{\eta}_r$) and lagoon ($\overline{\eta}_L$) drive a cross-reef current U_r over the reef. For fringing reefs, water flowing across the reef returns back to the ocean through channels in the reef (not shown).

radiation stress through the surf zone is partitioned between driving a cross-reef current and supporting a pressure gradient. *Symonds et al.* [1995] show how the relative magnitudes of the cross-reef current and pressure gradient depend on the width of the reef flat and the magnitude of the incident wave forcing for an idealized one-dimensional reef. In the two-dimensional case, the cross-reef volume flux must flow alongshore in the lagoon toward any channels in the reef (see below). This alongshore flow must also be forced by an alongshore pressure gradient, causing the lagoon sea level to increase in the lagoon and decrease toward the channel. The increase in lagoon sea level must in turn decrease the cross-reef pressure gradient and the corresponding cross-reef flow.

[3] Detailed experimental studies of wave-driven flows on coral reefs have been conducted using both physical laboratory models [e.g., *Gourlay*, 1996a, 1996b] and direct field observation [e.g., *Hench et al.*, 2008; *Lugo-Fernández et al.*, 2004; *Symonds et al.*, 1995]. To describe and predict these wave-driven reef currents, a number of semiempirical one-dimensional models have also been developed and have performed reasonably well for some coral reefs [e.g., *Gourlay and Colleter*, 2005; *Hearn*, 1999; *Symonds et al.*, 1995]. To date, most of these experimental and theoretical studies of wave-driven circulation in coral reefs have primarily focused on reefs with relatively deep and effectively unbounded lagoons, i.e., those reef systems with morphologies classified as 'barrier reefs' or 'atolls' [*Wiens*, 1962]. For these deep and/or open lagoon systems, studies have demonstrated that the dynamics of wave-driven currents are largely controlled by the morphology and physical roughness properties of the forereef and reef flat [*Gourlay and Colleter*, 2005], i.e., the morphology of the lagoon plays a minor role in the overall momentum dynamics. However, many coral reefs worldwide grow adjacent to a coastline, and thus have relatively shallow lagoons that are only free to exchange with the ocean through narrow gaps (channels) in the reef, i.e., those systems classified as 'fringing reefs' [*Kennedy and Woodroffe*, 2002]. Relatively few field studies have been conducted to investigate the dynamics of wave-driven flows generated within fringing reef systems. These studies have demonstrated that friction in the lagoons of fringing reefs can radically reduce the strength of wave-driven currents compared to those generated on atolls and barrier reefs, through a significant reduction in the cross-reef wave setup gradient $\overline{\eta}_r - \overline{\eta}_L$ (Figure 1). As a consequence, existing analytical models of reef circulation developed specifically for barrier reefs and atolls may not be directly relevant to predicting the circulation and flushing of fringing reef systems. Independent from the known morphological controls to reef circulation, analytical solutions have furthermore predicted that wave-driven currents on reefs should be sensitive to variations in the mean sea level over the reef flat; thus changes in water level over a tidal cycle should drive significant modulations in wave-driven currents, due to variations in radiation stress forcing and bottom friction [e.g., *Hearn*, 1999; *Symonds et al.*, 1995]. The importance of tidal modulations to these wave-driven flows has never been experimentally investigated on coral reefs, given that previous studies have either focused on the specific ebb-flood nature of the tides (i.e., draining/filling of the reef lagoon system) [e.g., *Kraines et al.*, 1999], the mean momentum dynamics (subtidal current variability) occurring on reefs [e.g., *Lowe et al.*, 2009b], or for particular reef systems where tides are virtually absent [e.g., *Coronado et al.*, 2007; *Hench et al.*, 2008].

[4] Here we investigate the dynamics of the circulation of Ningaloo Reef, located along the northwest coast of Western Australia (Figure 2), which at 290 km long is Australia's longest fringing coral reef system [*Cassata and Collins*, 2008]. Along this section of coast, shallow coral-dominated reefs (h_r ~1–2 m depth) grow ~1–6 km offshore and are separated from the coast by somewhat deeper, sedimentary lagoons (typically h_L ~2–5 m deep) [*Hearn et al.*, 1986]. Along its length, these shallow reefs are broken periodically by a number of gaps (channels) that allow water to exchange between the lagoon and open ocean; *Hearn and Parker* [1988] used aerial photographs of the northern part of the Ningaloo tract to estimate that these gaps occupy about 15% of its length. Relatively few studies have investigated the nearshore physical oceanography of Ningaloo Reef, but some unpublished data reports have suggested that breaking waves may generate much of the current variability occurring within the reef-lagoon system [e.g., *Brinkman*, 1998; *Hearn et al.*, 1986].

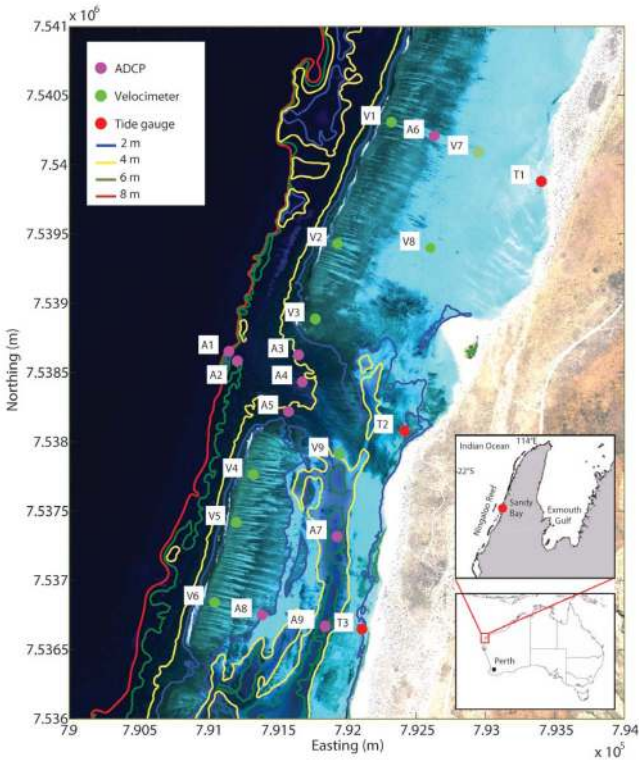

Figure 2. Map of the study area at Sandy Bay in Ningaloo Marine Park, located in the northwest of Australia (coordinates are based on UTM zone 49S). Isobaths between 2 and 8 m are superimposed to highlight the key features of the reef morphology. The locations of the moored instruments during the field experiment are also shown. The white bands visible along the reef crest show wave breaking, i.e., highlighting the narrow surf zone.

[5] The aim of the present study was to describe results from a 6 week field experiment at Ningaloo, in what perhaps represents the most extensive hydrodynamic field data set collected on a coral reef, in general (Table 1). The field study focused specifically on the dynamics governing circulation in a ~5 km section of Ningaloo Reef centered at Sandy Bay (Figure 2). This site was chosen because the reef appeared, from aerial photographs, to have morphological characteristics fairly representative of Ningaloo as a whole, with the measurement program focusing on a single channel with reef sections on either side. As shown below, the study area represents an individual reef-channel circulation cell; thus, when considered as a whole, the circulation of the entire 290 km Ningaloo Reef tract can be thought of as being composed of many of these functionally similar reef-channel circulation cells.

[6] This paper is organized as follows. A description of the study area, the field measurement program, and data analysis are described in section 2. The observations of waves, currents and mean water level variability are presented in section 3. This includes a detailed investigation of how the overall current variability is driven by both subtidal forcing mechanisms and through tidal fluctuations (via both direct and indirect means). In section 4, the relative importance of wave versus tidal forcing are discussed, and implications for flushing rates across the reef and lagoon are presented. Finally, a summary of the main results and conclusions of the study are described in section 5.

2. Field Experiment

2.1. Site Description

[7] The field experiment focused on an ~5 km section of Ningaloo Reef located in the Sandy Bay region of Ningaloo Marine Park (22° 13′S, 113° 49′E in Figure 2). The reef morphology at this site is typical of many parts of Ningaloo Reef, with a simple configuration of shore-parallel reef sections broken periodically by channels (gaps) in the reef. At Sandy Bay, the forereef slope (~1:30) rises to a shallow reef flat (mean depth ~1–2 m) covered by dense assemblages of coral (mostly tabulate *Acropora spp.*) [*Wyatt et al.*, 2010]. Waves break on the leading edge of the reef flat (i.e., at the reef crest) located ~1 km from shore. The L_r ~ 500 m wide reef flat is separated from shore by a deeper lagoon, comprised mostly of sand and coral rubble. The morphology of the lagoon differs significantly between the northern and southern regions of the study area: the northern lagoon is relatively shallow (mean depth ~2–3 m), whereas the southern lagoon is incised by a deep lagoon channel (mean depth ~8 m). The reef is broken at the center of the study site by a relatively deeper channel (mean depth ~5 m). Deeper channels in the reef are also present both north and south of the study area; these channels (not shown in Figure 2) are both located roughly 5 km on either side of the main Sandy Bay channel. The channel to the north is relatively narrow (~200 m), while the channel to the south is much more expansive (~1.5 km wide).

2.2. Data Sets

[8] An intensive 6 week field experiment was conducted during April and May 2006. During the experiment, 21 moored instruments were deployed at sites spanning from the forereef slope to the lagoon (Figure 2). Detailed sampling information for each instrument is included in Table 1 and only a summary follows. A RDI 600 kHz Workhorse Acoustic Doppler Current Profiler (ADCP) measured current profiles on the forereef at A1 (mean depth ~16 m). A 1 MHz Nortek AWAC directional wave gauge/current profiler was also deployed on the forereef at A2 (mean depth ~12 m), and measured both current profiles and the hourly directional wave spectrum using Acoustic Surface Tracking (AST). A 1 MHz Nortek Aquadopp current profiler was deployed within the Sandy Bay channel at A4 (mean depth ~5 m), and two 600 kHz RDI ADCPs were located further north and south within the same channel (A3 and A5). A series of Nortek Vector Acoustic Doppler Velocimeters (ADVs) were deployed along the reef flat (V1–V6), immediately shoreward of the surf zone, and sampled pressure and current velocities at a fixed height typically near the middle of the water column. Currents along the back reef and lagoon were measured using a series of 2 MHz Nortek Aquadopp current profilers and an Aquadopp current meter (A6 and A8; V7), while two InterOcean S4 single-point current meters were deployed at V8 and V9. Two 1200 kHz RDI ADCPs were also deployed in the relatively deep (mean depth ~8 m) southern lagoon (A7 and A9). Three RBR tide gauges (T1–T3) were deployed in the lagoon adjacent to the shore, and

Table 1. Instrument Locations, Configurations, and Deployment Information[a]

Site	Instrument	Depth (m)	Sampling Information	Measurement
A1 (forereef)	RDI 600 kHZ ADCP	16	Bin size = 0.5 m; Profile interval = 5 min	currents
A2 (forereef)	NORTEK 1MHZ AWAC	12	Bin size = 1 m; Currents: 15 min profile interval; Waves: 2048 samples at 2 Hz every hour	currents, waves
A3 (channel)	RDI 600 kHZ ADCP	5.3	Bin size = 0.5 m; Profile interval = 5 min	currents
A4 (channel)	NORTEK 1 MHz Aquadopp profiler	5.3	Bin size = 1 m; Currents: 15 min profile interval; Waves: 2048 samples at 2 Hz every hour	currents, waves
A5 (channel)	RDI 600 kHZ ADCP	4.4	Bin size = 0.5 m; Profile interval = 5 min	currents
A6 (reef flat)	NORTEK 2 MHz Aquadopp profiler	1.4	Bin size = 0.5 m Profile Interval = 10 min	currents
A7 (lagoon)	RDI 1200 kHZ ADCP	8.4	Bin size = 0.5 m; Profile interval = 15 min	currents
A8 (reef flat)	NORTEK 2 MHz Aquadopp profiler	2.2	Bin size = 0.5 m; Profile Interval = 10 min	currents
A9 (lagoon)	RDI 1200 kHZ ADCP	8.3	Bin size = 0.25 m; Profile Interval = 15 min	currents
V1 (reef flat)	NORTEK Vector ADV	1.9	Sample height = 0.5 m above bed Sampling: 4096 samples at 2 Hz hourly	currents, waves
V2 (reef flat)	NORTEK Vector ADV	1	Sample height = 0.15 m above bed Sampling: 300 samples at 1 Hz hourly	currents, waves
V3 (reef flat)	NORTEK Vector ADV	1.4	Sample height = 0.5 m above bed Sampling: 4096 samples at 2 Hz hourly	currents, waves
V4 (reef flat)	NORTEK Vector ADV	2.1	Sample height = 0.5 m above bed Sampling: 4096 samples at 2 Hz hourly	currents, waves
V5 (reef flat)	NORTEK Vector ADV	0.75	Sample height = 0.15 m above bed Sampling: 300 samples at 1 Hz hourly	currents, waves
V6 (reef flat)	NORTEK Vector ADV	1.4	Sample height = 0.5 m above bed Sampling: 4096 samples at 2 Hz hourly	currents, waves
V7 (lagoon)	NORTEK 2 MHz Aquadopp current meter	1.7	Sample height = 0.6 m above bed Current interval = 10 min	currents
V8 (lagoon)	InterOceans Systems S4 current meter	1.7	Sample height = 0.5 m above bed Current interval: 30 min	currents
V9 (lagoon)	InterOceans Systems S4 current meter	5	Sample height = 0.5 m above bed Current interval: 30 min	currents
T1 (lagoon)	Richard Brancker XR-420 tide gauge	1.5	Sample interval: 5 min	water level
T2 (lagoon)	Richard Brancker XR-420 tide gauge	1.5	Sample interval: 5 min	water level
T3 (lagoon)	Richard Brancker XR-420 tide gauge	1.7	Sample interval: 5 min	water level

[a]The instrument "depth" represents the mean water depth at each site recorded during the field experiment. Sites denoted with "A" refer to ADCPs measuring current profiles, sites denoted with "V" refer to velocimeters measured currents at single point, and sites denoted with "T" refer to tide gauges sampling pressure only.

sampled water level from recorded pressure. A series of thermistor chains were also deployed in the lagoon adjacent to the channel, to investigate vertical density stratification in the deeper regions (note that the system receives effectively no freshwater discharge from its arid coastline). Analysis of the thermistor records revealed the lagoon was well mixed throughout the experiment (not shown), so buoyancy effects were not considered in any subsequent analysis. During the study period, wind speed and direction was recorded every 30 min by a weather station operated by the Australian Institute of Marine Science at Milyering, on the coast approximately 20 km north of Sandy Bay. An estimate of the wind stresses were provided from the local wind speeds using surface drag coefficients from *Large and Pond* [1981].

2.3. Data Analysis

[9] Directional wave spectra were computed on the fore-reef (A2) using the Maximum Likelihood Method [*Emery and Thomson*, 2001] with the AST time series. For all shallower wave sites, one-dimensional surface elevation spectra $S(f)$ were derived from the pressure time series using linear wave theory. The elevation spectra were then used to calculate significant wave heights as $H_s = 4(m_0)^{1/2}$, where m_0 is the zeroth moment of $S(f)$ based on the energy between 2 and 30 s. The mean T_{m01} and peak T_p wave periods were subsequently calculated based on the first spectral moment of $S(f)$ and the spectral peak, respectively. Wave setup at each reef flat station (V1–V6) was estimated by subtracting the offshore water level at A2 (where setup and set down were estimated to be negligible) from the water level measured over the reef flat during the same time, applying the same approach detailed by *Lowe et al.* [2009b]. Hourly currents were obtained for each current meter by averaging all samples in a burst; for the ADCPs these were then averaged over all vertical bins to produce time series of the depth-averaged current velocities. To compare the depth-averaged currents measured by the ADCPs with those instruments measuring at a single point in the water column (e.g., the ADVs), the depth-averaged current was estimated from the point current measurements by assuming the velocity profile followed a simple 1/6 rough wall boundary layer power law [*Chanson*, 2004]. The conversion factor applied was typically very small (<10%), but was nevertheless included to provide a better estimate of the depth-averaged currents at each of the "V" sites (Table 1).

[10] Evaluation of the importance of each forcing mechanism (i.e., wave, wind, and tide) was quantified by computing correlation coefficients that related each forcing mechanism of interest to the local depth-averaged current measured at each site. Given that the response of the currents to waves, winds and tides may be frequency dependent, the spectral response of the currents to each forcing was also investigated. The currents and forcing variables were separated into both subtidal and intratidal components. The subtidal variability was assessed by low-pass filtering using the PL64 filter [*Beardsley et al.*, 1985] with a half-

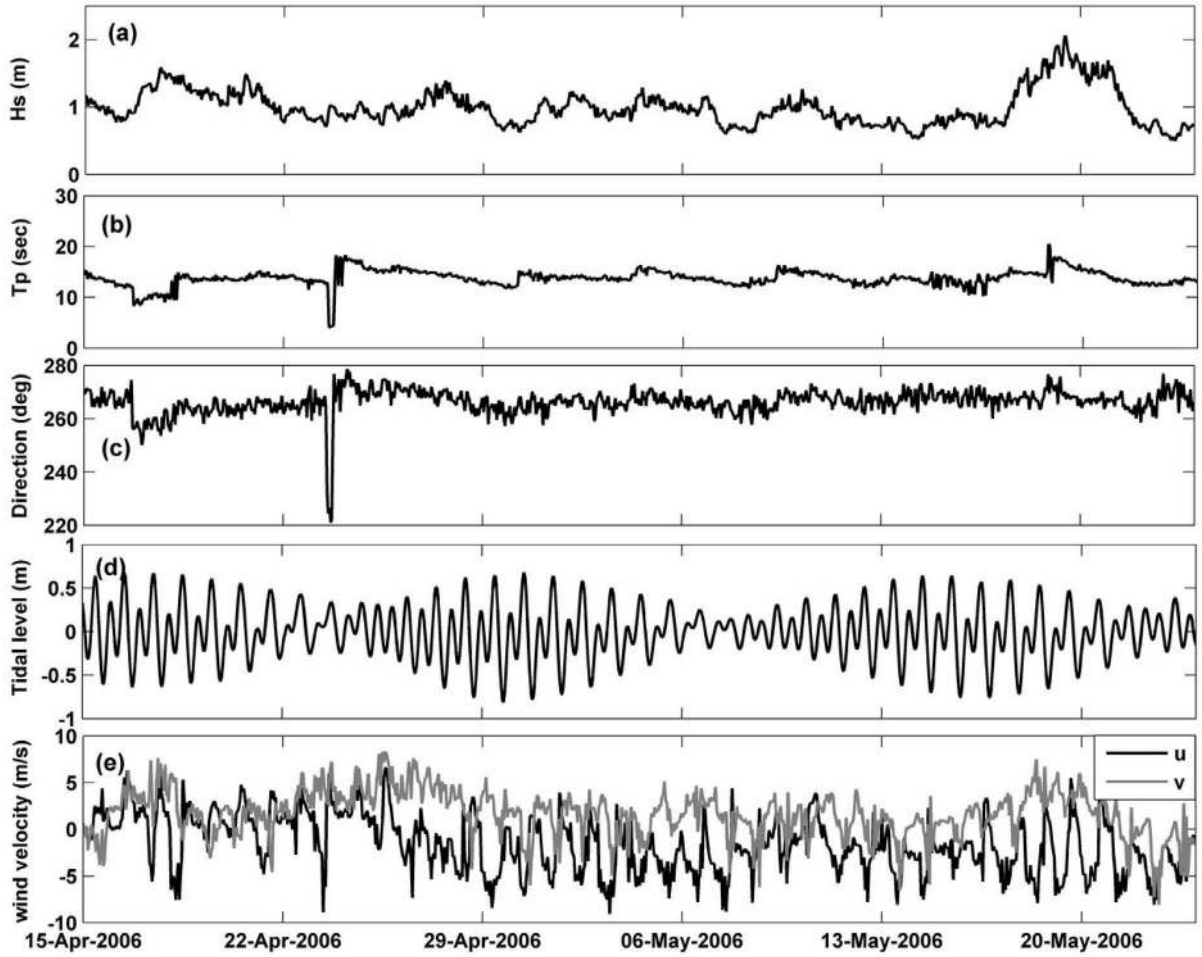

Figure 3. Oceanic and meteorological forcing conditions, observed during the field experiment. (a) Significant wave height H_s measured on the forereef at site A2. Corresponding (b) peak wave period T_p and (c) peak wave direction. (d) Hourly mean water level variability observed at A2 and (e) the wind velocity components measured at the Milyering weather station (note that positive u is directed eastward while positive v is directed northward).

power period of 38 h. The residual component (obtained by subtracting the subtidal signals from the original time series) was then referred to as the intratidal signal, and contained any variability with timescales shorter than 38 h (but greater than the hourly data sampling interval). The synoptic spatial response of the circulation patterns to temporal variability in forcing was evaluated using an empirical orthogonal function (EOF) analysis. For this analysis, the mean (time averaged) currents were not removed from the current time series, so the EOF analysis maximized total energy rather than just the variance of the data set [*Coronado et al.*, 2007].

3. Observations

3.1. Forcing Conditions

[11] The experiment captured a wide range of wave, tide and wind conditions. Offshore significant wave heights H_s incident to the forereef ranged between 0.5 m and 2.1 m, averaging 1 m (Figure 3a). The peak period T_p of the incident waves ranged from ~5 s (i.e., due to short-period wind waves) up to ~20 s associated with long-period swell events (Figure 3b). Throughout the experiment, waves were incident to the reef from a southwesterly direction (i.e., waves approaching normal to the reef would arrive from ~290°; see Figure 2).

[12] The experiment captured three spring-neap tidal cycles (Figure 3d) and three periods with fairly strong (>5 m/s) and continuous winds directed toward the north: these winds occurred in mid-April, toward the end of April, and mid-May (Figure 3e). The wind speed slowed down and changed direction frequently from the end of April to mid-May, and wave heights were also relatively small (H_s ~1 m) during this period.

3.2. Waves, Mean Water Levels, and Currents

[13] Wave heights measured at representative sites on the reef flat (V1 and V6) were significantly attenuated from forereef values (i.e., those measured at A2), due to depth-limited wave breaking over the shallow reef crest (Figure 4a). Moreover, the wave heights on the reef flat were also strongly modulated by tides, which changed the water depth over the reef crest and hence the amount of wave energy transmitted through the surf zone. As discussed in the introduction, the dissipation of wave energy within the surf

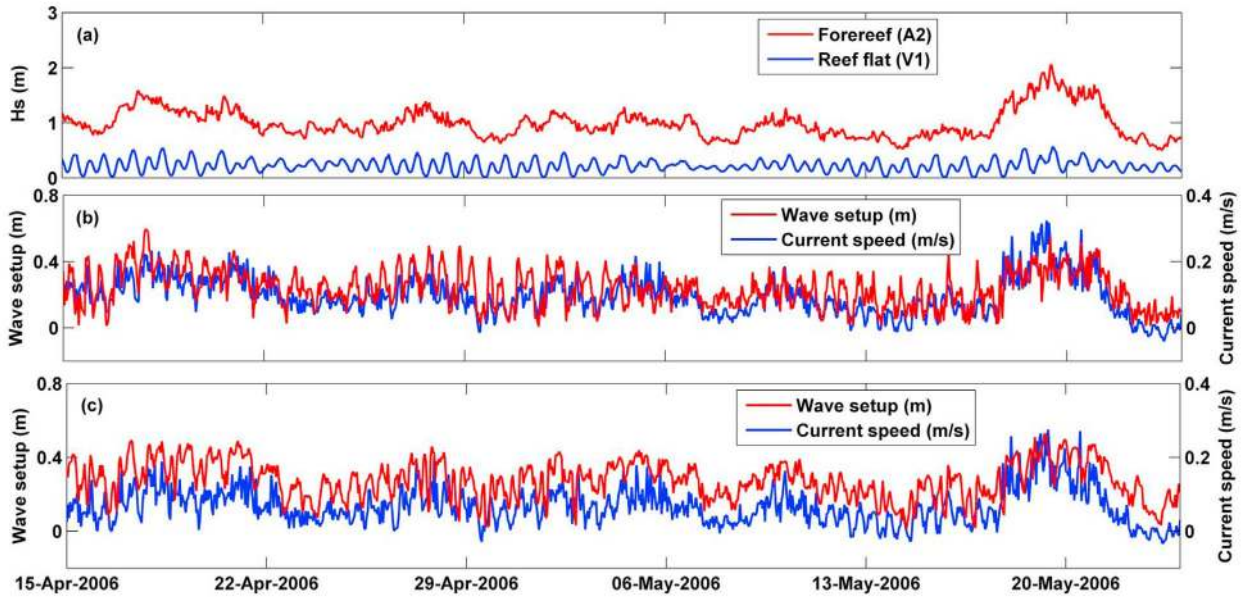

Figure 4. (a) Significant wave height for representative sites on the forereef (A2) and reef flat (V1). (b) Wave setup and current speed on the northern reef flat (V1). (c) Wave setup and current speed on the southern reef flat (V6).

zone generates setup at the seaward edge of the reef flat, with values as high as ~0.5 m when the significant wave height reached ~2 m offshore (Figures 4b and 4c). Furthermore, the lagoon sea level also increased, producing an alongshore pressure gradient to drive the flow toward the channel (see below). The response of wave setup $\overline{\eta}$ to the incident wave height was strongly correlated to the incident wave height, with the setup values near the reef crest comparable (but typically slightly greater) to values recorded within the lagoon during the same time (Figure 5).

[14] The time-averaged circulation pattern observed during the experiment (arrows shown in Figure 6), revealed a consistent shoreward flow across the reef flat (sites V1–V6), with a stronger return flow exiting to the ocean through the Sandy Bay channel (sites A3–A5). The flow associated with this channel jet extended at least 500 m offshore, as evident from the mean currents measured on the forereef (A1 and A2). Mean flow patterns on the back reef and within the lagoon were more complicated, with clear differences in the patterns occurring in the northern and southern regions. In the northern region, flow on the back reef (A6) and in the lagoon (V7–V8) contributed to the flow exiting the channel. The lagoon flow in the southern region was more complex, with the lagoon flow at V9 feeding the Sandy Bay channel, while those lagoon sites to the south (A7 and A9) fed a channel system south of the study area (not visible in Figure 6). Therefore, not all of the water crossing the southern reef flat actually returns to the ocean through the Sandy Bay channel, i.e., flow at V6 and likely V5 each contribute to the dominant southerly flow observed in the deep southern lagoon.

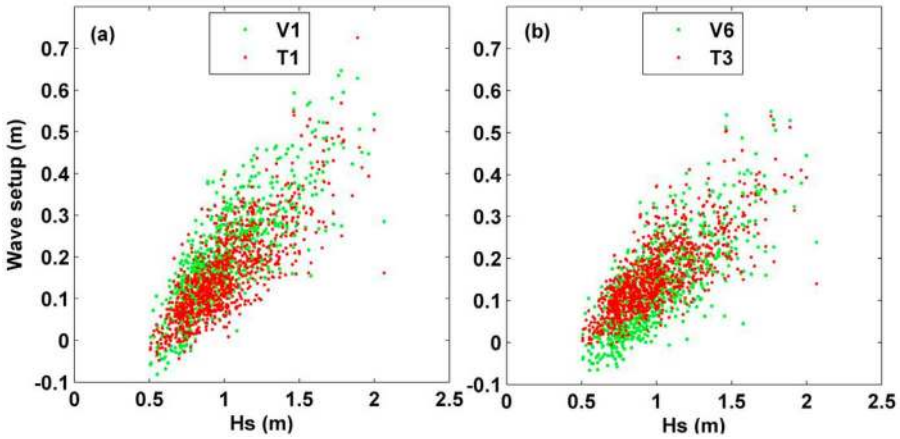

Figure 5. Wave setup recorded at (a) the northern reef flat (V1) and lagoon (T1) and (b) the southern reef flat (V6) and lagoon (T3), versus the incident significant wave height measured on the forereef (A2).

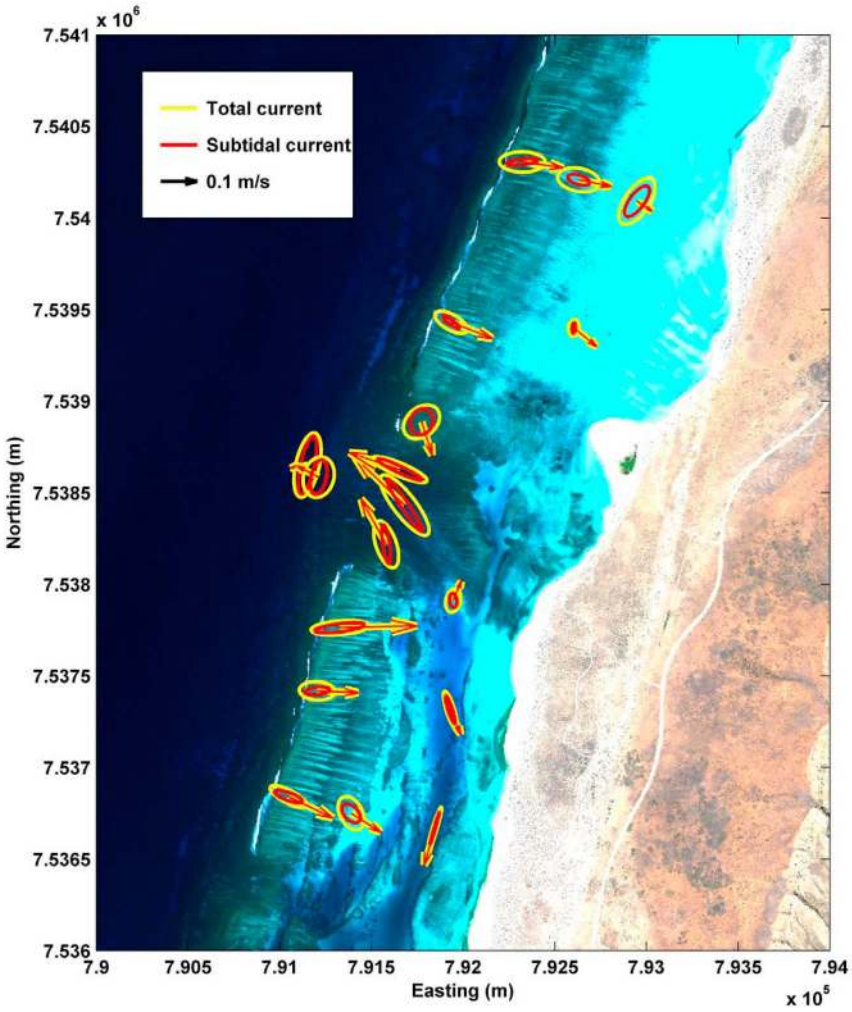

Figure 6. Circulation patterns and variability observed during the 6 week experiment. Arrows represent the time-averaged current vectors, while the ellipses represent 1 standard deviation of the current variability from a principal component analysis. The principal component analysis was conducted on both the original time series ("total current") and the 38 h low-pass filtered signals ("subtidal current"). Note that throughout the system, most of the current variance can be explained by variability occurring at the subtidal frequencies, i.e., the intratidal variability represented by the area between the ellipses is relatively small.

[15] The time series of the current speed U over the reef flat showed stronger subtidal current variations with a superposition of weaker tidal fluctuations (Figures 4b and 4c). The total current variability primarily resulted from changes in the incident wave energy, with correlation coefficients between the incident wave heights and current speeds ranging from R~0.5–0.9 for all sites on the reef flat, and R~0.8 for the channel flow (Figure 7). There was no significant correlation between the wind stress and current speeds observed at all sites (R~0.1), thus the subsequent analysis focuses on the dominant role that waves and tides play. While the currents increased in a monotonic fashion with increasing wave height, a more complex relationship is apparent between the currents and tidal variations. The correlation between the tidal elevation and current speed was relatively weak ($R <$ 0.3) at all sites, however, for the shallower reef sites (V1 and V6) a nonlinear (quadratic) response is clearly visible, which can partially explain the low linear correlation values (Figures 7d and 7f). This nonlinear response is most evident at the southern reef site (V6), where at high tides (+0.5 elevation) the flow is virtually absent, then increases as the tidal level is reduced, and then the flow again became negligible at lower tides (<−0.4 m). At these low tides, visual observations in the field indicate that the reef crest may become exposed in some parts (but not continuously along the reef crest), which would significantly limit any cross-reef flow. Thus for this site (V6) and to some degree at the northern site (V1), reef current speeds were at a maximum at some intermediate depth between high and low tide, i.e., an optimum appears to occur when the tide is 0.2–0.4 m below the mean water level. This feature of cross-reef currents was described by *Symonds et al.* [1995] and can result in the currents being modulated at twice the tidal frequency.

[16] Harmonic analysis of tidal levels using T_Tide [*Pawlowicz et al.*, 2002] showed that the maximum phase angle difference for the dominant M2 tide, computed

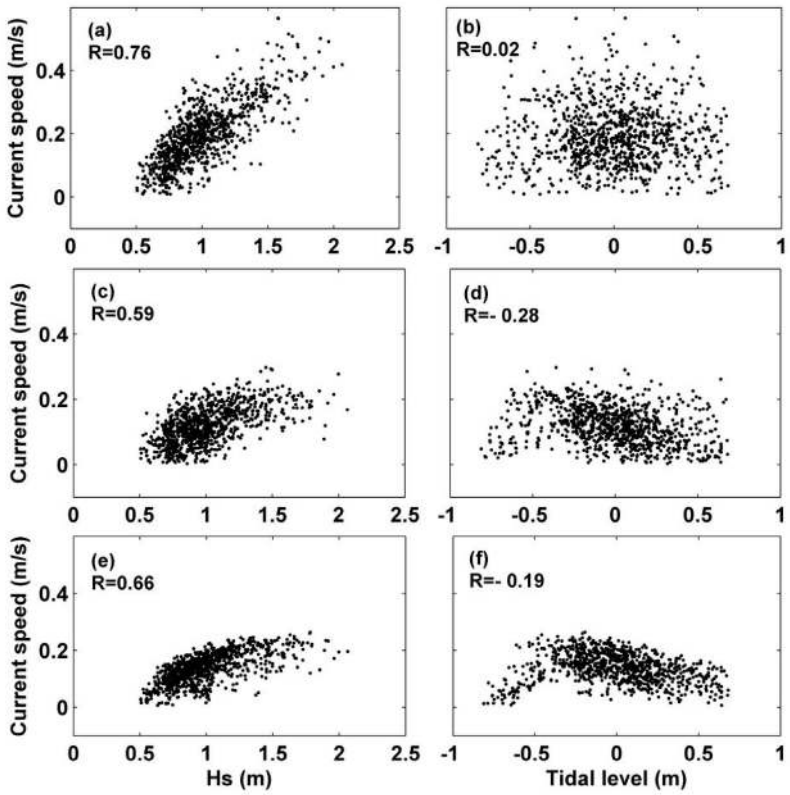

Figure 7. The response of the current speed (nonfiltered) to key forcing mechanisms (wave and tide), observed in the (a, b) channel A4, (c, d) northern reef flat V1, and (e, f) southern reef flat V6.

between the forereef site (A2) and all remaining sites on the reef flat and lagoon, was always less than 10° (and more typically less than 5°) (not shown). The tidal levels across the sites thus responded nearly synoptically over this relatively small nearshore study domain (of order 1 km).

3.3. Intratidal Variability

[17] Spectral analysis of the forcing variables (possible energy input to the system), revealed prominent diurnal and semidiurnal peaks in the water level time series due to the dominant tidal constituents, a small diurnal peak in wind stress associated with the sea breeze cycle, and no prominent peaks in the wave height record (Figure 8a). The resulting wave setup and cross-shore current response on the reef at V1 showed prominent semidiurnal and diurnal peaks, with some weaker higher-frequency harmonics (Figure 8b). The ratios of the spectral amplitudes between different key frequency components were calculated from the tidal level and cross-shore current spectra (see Table 2). For tidal level, the energy was dominated by semidiurnal variability with virtually no energy at tridiurnal and quarterdiurnal harmonics (i.e., the amplitudes of these harmonics are <0.1% of the diurnal amplitude). However, variability in the cross-shore currents was much more uniformly distributed among the frequency components, with much more current energy was contained within the higher-frequency constituents (i.e., their amplitudes are ~10% of the diurnal peak).

[18] A spatial EOF analysis was applied to both the low-pass (subtidal) and high-pass (intratidal) reef flat and channel current time series. The first mode of the subtidal currents shows shoreward flow over the reef flat and a return flow exiting the channel (Figure 9a). This first subtidal mode explains virtually all of the observed subtidal variance (96%), i.e., the variance explained by the second mode is negligible (<3%). The amplitude of the first subtidal mode in Figure 9b was strongly correlated with the incident wave height at A2 (R = 0.92). The positive sign of its amplitude indicates the circulation associated with this subtidal mode was always in the direction of the vectors shown in Figure 9a, i.e., this flow pattern never reversed.

[19] Conversely, the vectors associated with the first mode of the intratidal currents were either all directed onshore or all directed offshore (Figure 9a), depending on the sign of the oscillating modal amplitude (Figure 9b); this first mode only explained a somewhat limited amount (~40%) of the intratidal variance. The magnitude of the mode 1 intratidal vectors also varied across the domain, with generally much stronger flow through the channel relative to over the reef flat. This variability appears to be due to the preferential tidal flow through the deeper channel, where it experiences less frictional resistance compared to the shallow reef flat – a similar response has also been observed within other coastal reef-lagoon systems [e.g., see *Lowe et al.*, 2009b]. We also note the magnitude of the intratidal mode 1 flow on the northern reef flat (V1) flat is much larger than on the southern reef flat (V4 and V6). This may be due to the fact that both the southern reef sites are quite close to channels, which may cause the flow to bypass to the nearby deeper

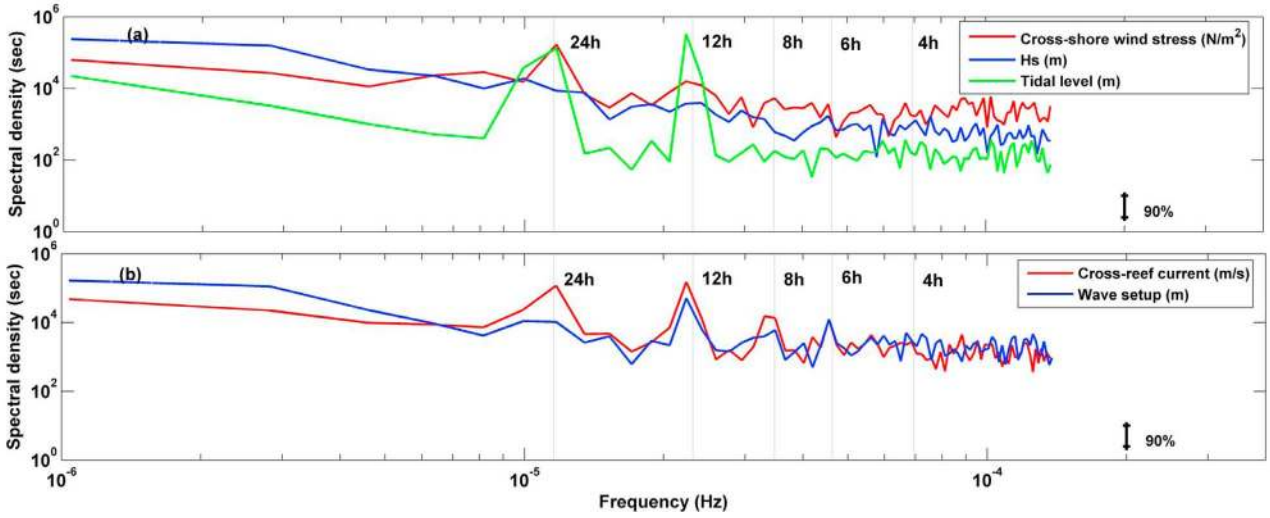

Figure 8. Normalized autospectral densities for (a) various forcing mechanisms (cross-shore wind stress, forereef wave height, and tidal level) and (b) the response variables measured at V1 (wave setup and cross-reef current). Each spectrum is normalized by the total energy in the spectrum to compare different variables (with differing units).

channel regions – for the northern site, a large channel is located quite a large distance away (1+ km). The northern site also appeared to be deployed in a large groove in the reef which may also contribute to its greater tidal flow (see Figure 1). The variance explained by the second mode of the intratidal signal was much greater (20%; see Figure 11) than the corresponding second mode of the subtidal signal. The vector field of this second intratidal mode closely resembled the wave-driven flow pattern (i.e., has a similar pattern to the first mode of the subtidal signal; see Figure 9a), with shoreward flow across the reef flat and a return flow exiting the channel (Figure 11a). Moreover, results from a lag correlation analysis predicted a maximum correlation (R = 0.38) existed when this modal amplitude led the tidal elevation by +6 h. This is half of the dominant semidiurnal period (6 h), or equivalent to a roughly 180° phase lag between this second modal amplitude and the tidal elevation, i.e., suggesting that these currents were at a maximum when the tidal elevation was at a minimum.

4. Discussion

[20] The field observations focused on a morphologically typical section of Ningaloo Reef, characterized by two shallow reef segments (northern and southern) that were broken by a deeper channel. This study thus focused on the dynamics of just one reef-lagoon-channel circulation cell, whereas the entire ~290 km long Ningaloo Reef tract would be composed of up to a hundred analogous circulation cells; therefore, the results from this study have broader implications for our understanding of how circulation is driven within Ningaloo Reef as a whole. The currents in the study area were dominantly wave driven, yet influenced (both directly and indirectly) by the tides. Winds had a very minor influence on the reef circulation (despite periods of strong winds up to ~10 m/s), and buoyancy effects were also negligible. While the dynamics of any larger-scale (regional) currents occurring off the reef were not the focus of the present study, they also appeared to have very little influence on the circulation inside the reef itself, i.e., despite the significant alongshore current variability observed on the forereef (A1 and A2), nearly all of the current variability inside the reef was driven by incident wave forcing and tides alone.

Table 2. Relative Amplitude of Tidal Level and Cross-Shore Current on the Reef at V1 for Different Tidal Frequency Component Ratios

Ratios	Tidal level	Cross-Shore Current
Semidiurnal/diurnal	2.50	1.28
Tridiurnal/diurnal	0.0005	0.10
Quarterdiurnal/diurnal	0.0006	0.08

4.1. Wave-Driven Circulation

[21] Forcing provided by wave breaking was able to explain much of the total current variability (R for all sites averaged ~0.6), and the bulk of the subtidal variability (R for all sites averaged ~0.8). Results from the EOF analysis of the subtidal currents revealed a dominant mode 1 pattern that closely resembled the mean wave-driven flow patterns, with this mode alone explaining 96% of the subtidal current variance. In general, these wave-driven currents appeared to increase linearly with increasing incident wave height, following the scaling predicted from 1-D analytical models of wave-driven currents generated on reefs [e.g., *Hearn*, 1999; *Symonds et al.*, 1995]. While wave-driven flows have been observed on many coral reefs, most of these studies have focused on atolls and barrier reef systems with relatively open and expansive lagoons, i.e., lagoons capable of exchanging readily with the open ocean [e.g., *Gourlay and Colleter*, 2005; *Hench et al.*, 2008; *Symonds et al.*, 1995]. For these open lagoon systems, strong wave-driven currents (up to 1 m/s) can be generated over the reef [e.g., see *Gourlay and Colleter*, 2005] due to a large water level (wave setup) difference that can be established between the

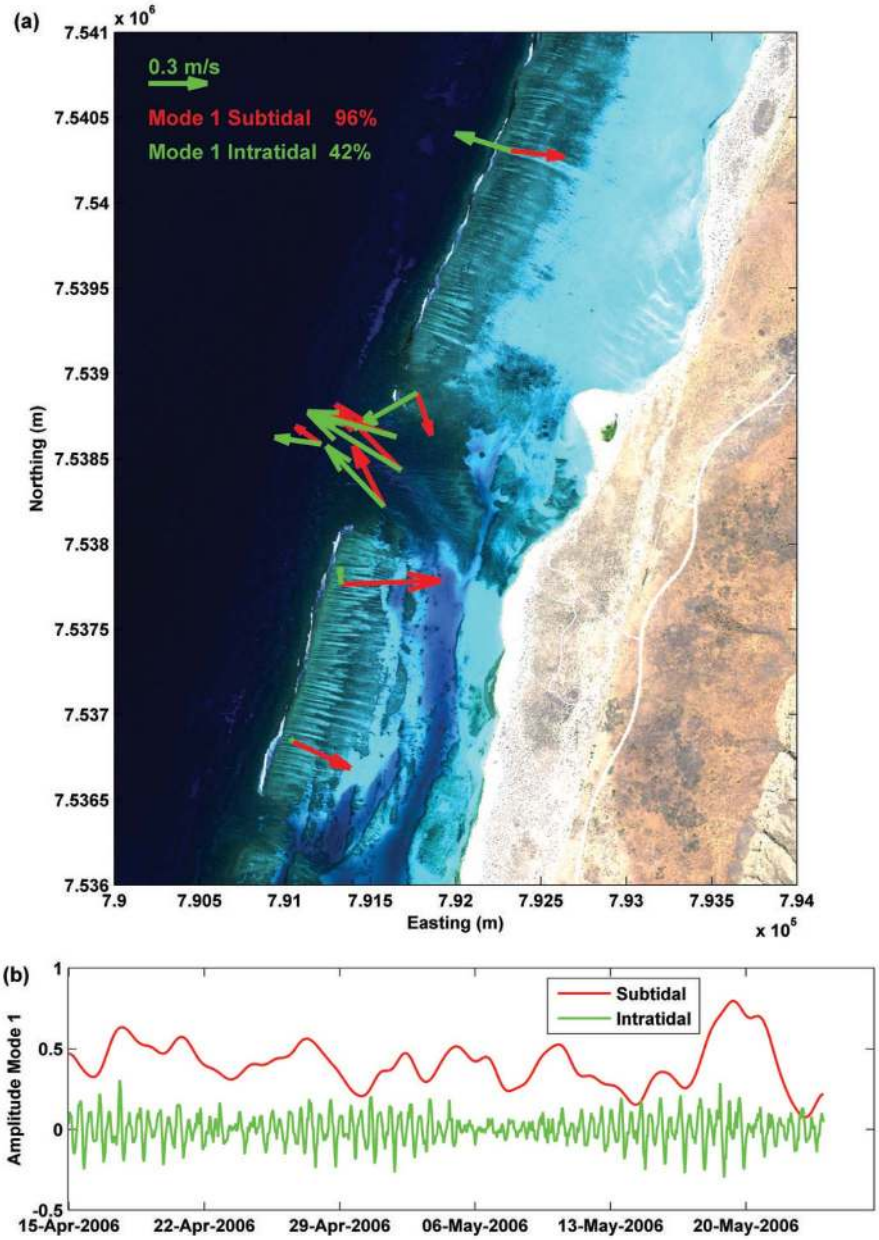

Figure 9. First EOF mode of current variability for both subtidal and intratidal components. (a) Spatial structure of the first mode and (b) the time series of the first modal amplitudes.

reef crest and the lagoon, where the lagoon setup in this case is almost zero, or roughly equal to the open ocean sea level. For coral reefs such as Ningaloo, having lagoons bounded by a shoreline (i.e., those classified as fringing or coastal reefs), inflow over the reef flat must flow along the lagoon and exit through the channels. This alongshore flow in the lagoon is forced by an alongshore pressure gradient which requires setup in the lagoon that decreases toward the channel. The presence of this lagoon setup can significantly reduce cross-reef water level gradients, which consequently limits the magnitude of the flow across the reef flat. The influence of this lagoon setup is particularly striking when comparing the differences in the wave-driven flow response, between Ningaloo and other systems having relatively open lagoons, such as at Moorea [*Hench et al.*, 2008], which has comparable reef flat dimensions. For the Moorea system, maximum reef crest setup values of only ~0.2 m generate wave-driven reef currents in excess of 0.5 m/s. In contrast, despite the reef crest setup we observed at Ningaloo being much greater (up to 0.5 m), currents of only 0.2–0.3 m/s were observed. The influence of lagoon morphology on wave-driven currents has not been considered in existing 1-D analytical reef circulation models [e.g., *Gourlay and Colleter*, 2005; *Symonds et al.*, 1995], however, the influence of finite lagoon setup in fringing reefs can be incorporated within these models, (e.g., following *Lowe et al.* [2009a]).

[22] Even within the same study site, variability in lagoon morphology led to some significant spatial differences in the wave-driven flow patterns that were generated. For this section of Ningaloo Reef, the cross-sectional area of the

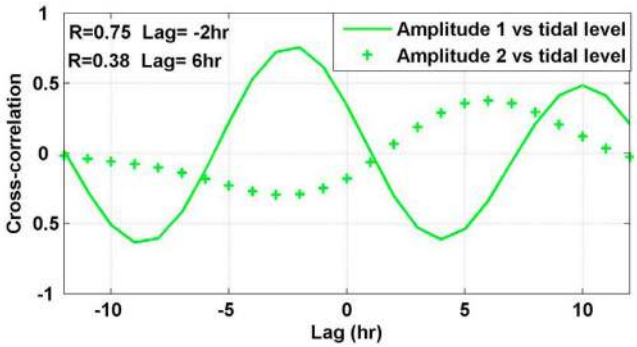

Figure 10. Lag correlation between time series of tidal elevation and both the EOF mode 1 and mode 2 amplitude time series.

northern lagoon is much less than the southern lagoon. Therefore, to maintain the same alongshore volume flux, a larger alongshore pressure gradient is required in the northern lagoon causing greater lagoon setup which in turn reduces the cross-reef volume flux. As a consequence, the wave-driven currents on the northern reef flat were generally weaker than those occurring across the southern reef flat (on average 25% lower; see Figure 6). Finally, the deeper channel in the southern lagoon is partially blocked by a shallow sill near the central channel causing some of the cross-reef flow to turn south at sites A7 and A9. This southward flow returns to the ocean through a major channel (~1.5 km wide by 9 m deep; not shown in Figure 2), which is located some 3 km south of V6. Therefore, while the channel that is the focus of this study (A4) is much closer to V6 (it is only ~1.5 km away), water in the southern lagoon A7 and A9 flows to the south, thus driven to exit a much more expansive channel.

4.2. Tidal Influence

[23] Tides interacting with shallow reefs have the potential to generate current variability at tidal frequencies via at least the following two mechanisms: (1) the ebb-flood cycle which moves water on and off the reef and (2) tidal modulations to any wave-driven currents present. Unfortunately, given that both of these processes generate current variability at similar frequencies, decomposing the contribution made by these two processes from reef current records has proven challenging; indeed the importance of the latter mechanism (tidal modulation of wave-driven currents) has only been predicted from 1-D analytical models of wave-driven reef circulation, which have investigated the potential response of flow to the mean water level over the reef crest [e.g., *Hearn*, 1999; *Symonds et al.*, 1995].

[24] Although the empirical modes returned by an EOF analysis of ocean current fields may not always correspond to distinct modes of dynamical significance [see *Emery and Thomson*, 2001], the results from the EOF analysis of the intratidal currents in this study do suggest that it provides an effective means to isolate the response of these two potential tidal forcing mechanisms. From this analysis, the first mode of the intratidal signal appears to be driven by the standard ebb-flood cycle of the tide. This is supported by the orientation of the intratidal mode 1 flow vectors, with the vectors all directed either onshore or offshore (i.e., consistent with the filling or draining of the lagoon by the tide). In addition, given that the tidal currents may not be in phase with water elevation in shallow water, a lag correlation analysis was also conducted on the intratidal mode 1 amplitude time series (Figure 10), this gave a maximum correlation (R = 0.75) when this mode lagged the water elevation by 2 h. In shallow coastal systems, the phase difference between tidal currents and water levels typically varies between 0° and 90°. In the limit of a small bay having a relatively large entrance, there is effectively no phase difference between the tidal elevation in the sea and the bay; as a result, there is almost zero flow at high and low tide (i.e., the elevation and currents are 90° out of phase) characteristic of a standing wave. Conversely, in the limit of a larger bay with relatively narrow inlets, the maximum water elevation inside the bay will occur later than in the sea, implying that flow will continue to enter the bay at high tide; therefore, the current will be out of phase by some value less than 90° [e.g., *Kamphuis*, 2000]. The relatively small phase difference (typically <10°) in the tidal levels observed between sites inside and outside the reef would suggest that the tide functions as a standing wave within this reef-lagoon system (see section 3.2). With the mode 1 amplitude of the intratidal currents lagging the water level by ~2 h, this would also correspond to a phase angle difference of ~60° between the currents and water levels for the dominant semidiurnal tide. Although this observed phase difference between the currents and tidal levels is slightly lower that the phase difference expected for a pure standing wave (90°), these separate observations offer further support that the tide functions as a standing wave (as opposed to a progressive wave having a phase difference of 0°) within this particular reef-lagoon system.

[25] Conversely, the EOF mode 2 vectors of the intratidal currents were observed to closely resemble the subtidal wave-driven current patterns (Figure 6). This mode thus appears to represent the distinct contribution made by the tides in modulating the wave-driven currents. This is further supported by the intratidal mode 2 response, with the phase difference of the mode 2 amplitude leading the water level by ~6 h, or equivalent to a 180° phase angle difference based on the dominant semidiurnal tide (Figure 3). This implies that the maximum amplitude of this mode is greatest when the water level is at its lowest, thus consistent with how wave-driven currents have been theoretically predicted to respond to tidal variations [i.e., *Hearn*, 1999; *Symonds et al.*, 1995]. We note that such a correlation analysis does assume a linear response between the variables, which is not strictly the case, i.e., Figures 7d and 7f showed that at very low tides the reef currents drop off rapidly. This degree of nonlinearity in the response likely explains why the maximum correlation for mode 2 is somewhat lower than for mode 1, and perhaps can account for the presence of the negative current spikes in the mode 2 amplitude time series at very low tides (see Figure 11b). However, for the bulk of the tidal cycle (tidal level >−0.4 m), the reef currents do indeed increase as water depth decreases (consistent with a linear response). These results thus strongly suggest that the mode 2 intratidal signal incorporates the dominant dynamics of the tidal modulations to the wave-driven currents.

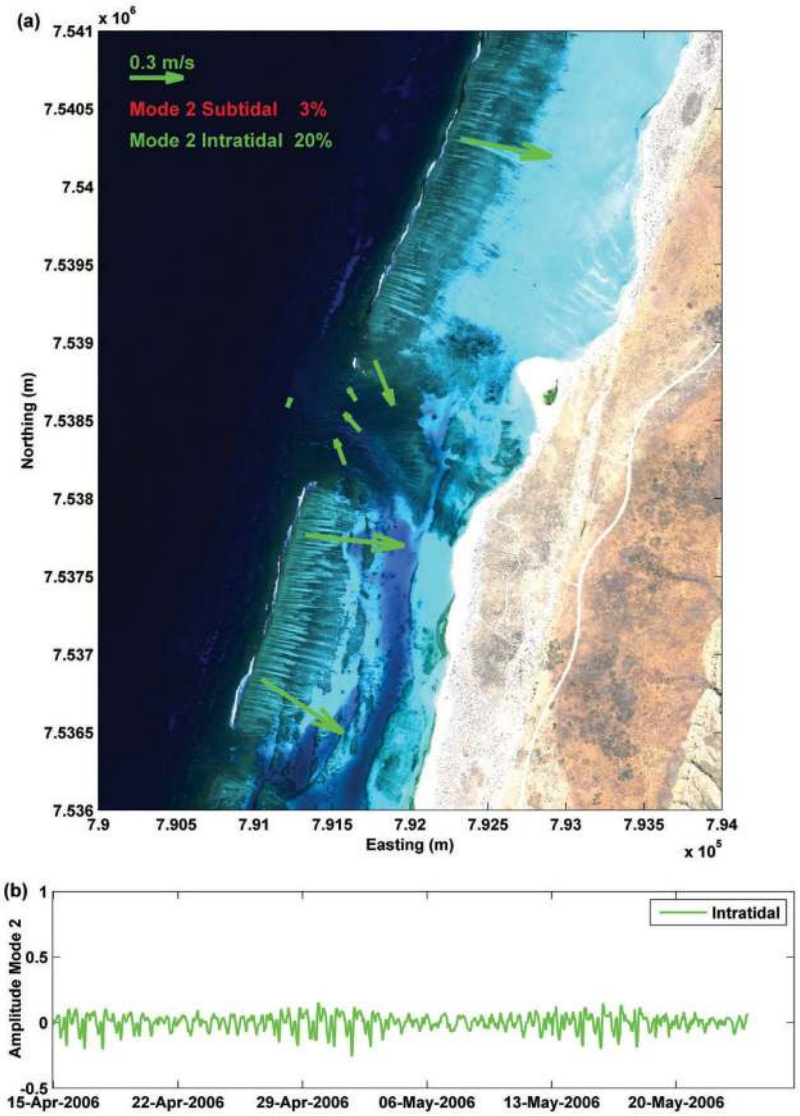

Figure 11. Second EOF mode of the intratidal current variability (note that the mode 2 subtidal results are not shown due to its trivial contribution to the subtidal currents). (a) Spatial structure of the second mode and (b) the time series of the modal amplitude.

[26] Based on this evidence, we can compare these two intratidal modes to provide an estimate of the relative importance of these two tide-driven mechanisms. For sites on the reef flat (V1, V3, V4, V6), the standard deviation of the variability in modes 1 and 2 were 0.026, 0.033, 0.008, 0.002 m/s and 0.031, 0.016, 0.034, 0.033 m/s, respectively. The variability of first mode (ebb-flood cycle of the tide) is larger in the northern reef, while for the second mode (modulations in the wave-driven currents), the southern reef shows greater variability (e.g., Figures 9 and 11). This indicates that the intensity of these intratidal modes varies from differences in reef/lagoon geometry, i.e., the tidal modulations in wave-driven currents are stronger in the southern reef section, presumably due to the more expansive (less constrained) nature of its lagoon.

[27] The wave-driven currents on the reef flat show a nonlinear (parabolic) response to changes in tidal depth, i.e., there exists an optimum depth to generate maximum wave-driven flow (Figures 7d and 7f). This trend is consistent with theoretical 1-D model predictions of wave-driven flows on coral reef flats [e.g., see *Symonds et al.*, 1995, Figures 8 and 10]. The one-dimensional momentum equation for wave driven cross-shore flow (neglecting convective accelerations) is given by

$$g\frac{\partial \overline{\eta}}{\partial x} + \frac{1}{\rho(h+\overline{\eta})}\frac{\partial S_{xx}}{\partial x} + \frac{C_D|q|q}{(h+\overline{\eta})^3} = 0, \qquad (1)$$

where x is the cross-reef axis perpendicular to the reef, q is the volume flux per unit width, i.e., $q = U(h + \overline{\eta})$, h is water depth relative to offshore mean sea level, ρ is density of seawater, S_{xx} is the wave radiation stress and C_D is the drag coefficient based on a quadratic drag law. Through the surf zone the radiation stress gradient (second term) is balanced by bottom friction (third term) and a pressure gradient (first term). Just how the radiation stress forcing term is partitioned

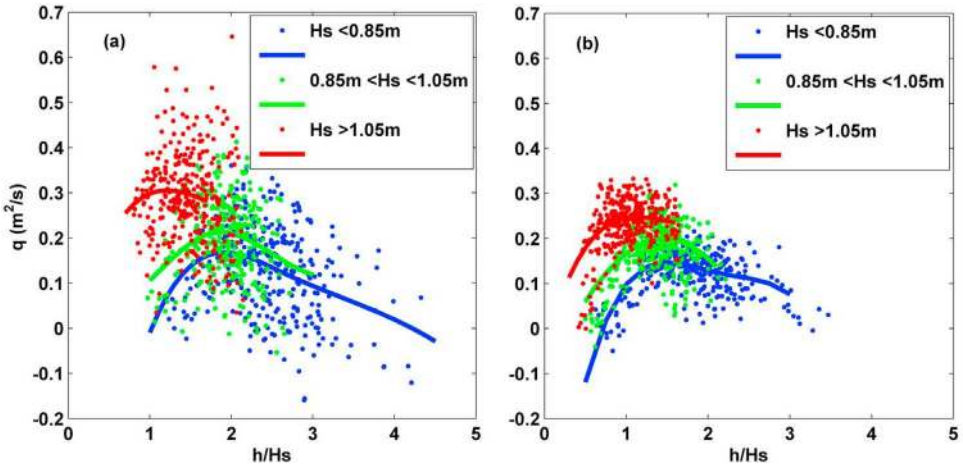

Figure 12. Volumetric flow per unit reef width q measured (a) on the northern reef flat at V1 and (b) on the southern reef flat at V6, versus the normalized water depth. Results are binned according to three wave height ranges. The solid lines highlight the average trends within each data set (obtained using a cubic spline interpolation).

between friction and the pressure gradient depends on the geometry of the reef and the magnitude of the incident waves. On the reef flat shoreward of the surf zone, the radiation stress gradient is effectively zero and the flow is driven by the pressure gradient only.

[28] With constant offshore wave forcing, radiation stress gradients in the surf zone will decrease via equation (1) as the depth increases over the reef (i.e., as indicated by the tidal modulation in reef wave heights in Figure 4a). As the depth decreases to zero, the cross-reef flow must also vanish. This leads to the result that the cross-reef flow is a maximum at some intermediate depth causing a modulation of the cross-reef flow at twice the tidal frequency, i.e., as reported by *Symonds et al.* [1995] and *Kraines et al.* [1998].

[29] For field conditions, both offshore wave height and tidal elevation covary, thus to isolate the response of tides, results were binned into different wave height ranges with the dimensionless group picked from *Symonds et al.* [1995]. Figure 12 suggests that for most wave bands there was a certain ratio of reef depth to wave height (h/H_s) that generated maximum volumetric flow q over the reef flat, i.e., this response is analogous to Figure 12b in *Symonds et al.* [1995]. This optimum ratio h/H_s varied from ~2 for small wave conditions ($H_s < 0.85$ m) to ~1 for larger wave conditions ($H_s > 1.05$ m). Very small or big ratios of h/H_s generate negligible q over the reef. For large h/H_s, wave breaking at the reef crest may be absent or substantially reduced, resulting in negligible reef wave setup and cross-reef flow. For small h/H_s significant wave breaking would occur, however, the relative water depth is shallow resulting in increased friction experienced by the cross-reef flow and perhaps even flow being blocked as the reef crest becomes partially exposed.

4.3. Flushing Time Estimates

[30] A variety of derived hydrodynamic parameters can be defined to estimate the rate at which a coastal system, such as Ningaloo Reef, exchanges water with the ocean [e.g., see *Monsen et al.*, 2002]. In coral reef studies, the 'residence time' in a lagoon is typically defined to be the time it takes for a water parcel to exit the lagoon to the ocean, e.g., by leaving through a channel in the reef [*Tartinville et al.*, 1997]. The 'flushing time' or 'turnover time' is instead represented by spatially averaging the residence time over the volume of water in the lagoon. Spatially explicit maps of residence time can only be obtained via numerical modeling and particle tracking [e.g., *Lowe et al.*, 2009a]; however, we can apply the field data to provide some estimate of the lagoon flushing time, and most importantly how this time responds to changes in physical forcing. We thus estimate the flushing time T_f of the lagoon region as [e.g., *Fischer et al.*, 1979]

$$T_f = V/Q_L, \tag{2}$$

where V is the volume of water in the lagoon and Q_L represents the flow (in m^3/s) of water from the lagoon to the

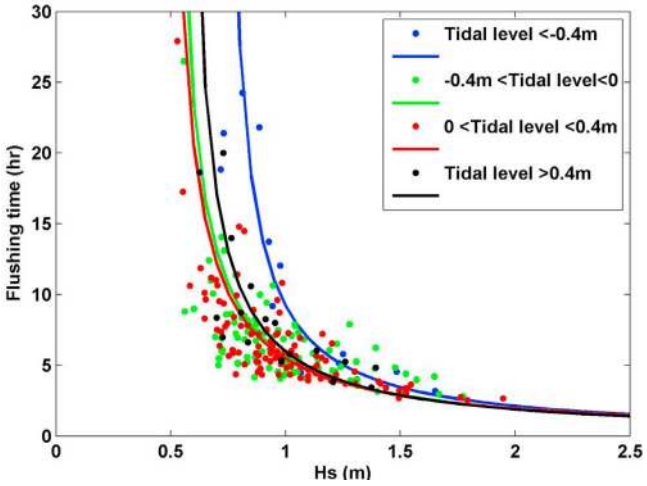

Figure 13. Flushing times estimated from equation (2) versus the incident wave height H_s binned for tidal elevation. The lines show the best fit proportional to H_s^{-1}.

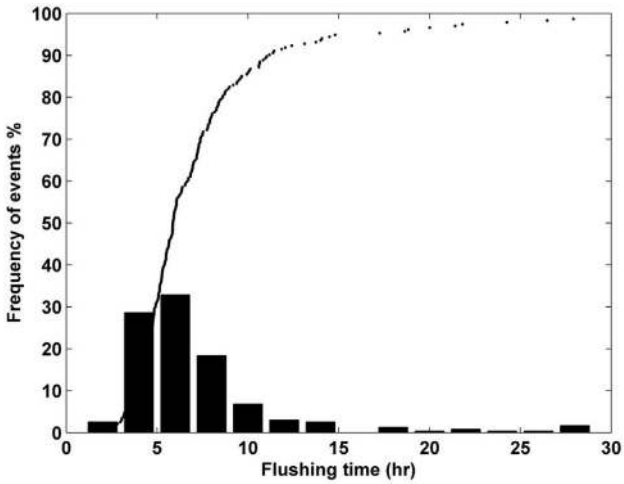

Figure 14. Flushing time histogram from the 6 week experiment, with the cumulative probability distribution superimposed.

ocean, i.e., estimated from the flow exiting the study area, measured in channel at A3–A5 and in the southern lagoon at A9. We note that equation (2) effectively assumes that any water exiting the channels does not become reentrained into the reef system [*Monsen et al.*, 2002], and as such, the rate estimated by equation (2) would represent a minimum flushing time for this system.

[31] High-resolution bathymetry for Ningaloo, derived from hyperspectral imagery (3.5 m horizontal resolution, <10% RMS depth error) was used to compute both the lagoon volume and cross-sectional areas of the exit channels. The lagoon volume included all of the water enclosed shoreward of the reef crest (i.e., this included the reef flat), and incorporated changes in the volume due to tides and wave setup. By integrating the channel and lagoon currents (A3–A5 and A9) over the total channel cross-sectional area, the flow rate Q_L was evaluated; from this, a time series of the flushing time T_f for this section of Ningaloo was computed. Given the importance of wave-driven currents, T_f depended strongly on the incident wave height, ranging from >1 day when the waves were small, to as fast as 3 h when wave heights were ~2 m (Figure 13). The flushing time also depended on the tidal elevation, especially when wave conditions were small, with the flushing time increasing when the water level was altered from present mean sea level. The cumulative histogram in Figure 14 shows that the median flushing time during the experiment was ~6 h, i.e., suggesting that the system typically exchanges water with the ocean at a rate equivalent to more than 4 times its volume each day.

5. Conclusions

[32] The results from a 6 week field experiment revealed that the circulation within a representative section of Ningaloo Reef was dominantly driven by the effects of wave breaking, with tides playing a secondary but significant role. Both winds and the presence of regional currents offshore had a negligible influence on circulation during the course of the study, both on the reef and within the lagoon. Although the response of the reef wave setup to the incident wave forcing was comparable with observations in other reef systems, the currents generated on the reef flat were comparatively weak (<0.2 m/s). This was due to the substantial setup in the lagoon, which significantly reduced the cross-reef water level difference between the reef and the lagoon responsible for driving the wave-driven flows.

[33] Intratidal current variability on the reef was driven by a combination of the ebbing/flooding of the system, as well as the modulation of the wave-driven currents with changes in water depth. Results from an EOF analysis of the intratidal current indicated that each mechanism is of comparable importance in driving the overall current variance observed at tidal frequencies. Results from the spectral analysis suggested that current harmonics were excited at some frequencies not limited to those in the water level harmonics; this is consistent with the generation of wave-driven current harmonics predicted theoretically by *Symonds et al.* [1995]. Also consistent with the theory, the strength of the wave-driven currents and flushing in this mesotidal system are clearly strongly dependent on the water level over the reef flat. Due to the opposing response of wave setup gradients and bottom friction to changes in water depth, the dominant terms in the reef momentum balance lead to the existence of an optimum mean water level that generated maximum wave-driven flow. For the reef at Ningaloo, this optimum depth appears to occur for water levels less than roughly 30 cm below present mean sea level. As a consequence, these results suggest that even a moderate climatological sea level rise would lead to a reduction in the wave-driven circulation and flushing of this reef-lagoon system.

[34] **Acknowledgments.** Funding for this project was provided by a grant to the authors from the Western Australian Marine Science Institution (node 3.5) and an Australian Research Council Discovery grant DP0770094 to R.J.L. We also thank W. Klonowski and M. Lynch of Curtin University for providing access to their processed hyperspectral bathymetry data for the region.

References

Atkinson, M. J., and J. L. Falter (2003), Biogeochemistry of coral reefs, in *Biogeochemistry of Marine Systems*, edited by K. P. Black and G. D. Shimmield, pp. 40–64, CRC Press, Boca Raton, Fla.

Beardsley, R. C., R. Limeburner, and L. K. Rosenfeld (1985), Introduction to the CODE-2 moored array and large-scale data report, in *CODE-2: Moored Array and Large-Scale Data Report*, edited by C. A. Alessi et al., pp. 1–36, Woods Hole Oceanogr. Inst., Woods Hole, Mass.

Bowen, A. J., D. L. Inman, and V. P. Simmons (1968), Wave 'set-down' and set-up, *J. Geophys. Res.*, *73*, 2569–2577, doi:10.1029/JB073i008p02569.

Brinkman, R. M. (1998), Data report: Ningaloo Reef (November–December 1997), technical report, Aust. Inst. of Mar. Sci., Townsville, Queensl., Australia.

Cassata, L., and L. B. Collins (2008), Coral reef communities, habitats, and substrates in and near sanctuary zones of Ningaloo Marine Park, *J. Coastal Res.*, *24*, 139, doi:10.2112/05-0623.1.

Chanson, H. (2004), *The Hydraulics of Open Channel Flow: An Introduction; Basic Principles*, 2nd ed., 585 pp., Elsevier, London.

Coronado, C., J. Candela, R. Iglesias-Prieto, J. Sheinbaum, M. López, and F. J. Ocampo-Torres (2007), On the circulation in the Puerto Morelos fringing reef lagoon, *Coral Reefs*, *26*, 149–163, doi:10.1007/s00338-006-0175-9.

Emery, W. J., and R. E. Thomson (2001), *Data Analysis Methods in Physical Oceanography*, 2 ed., 638 pp., Elsevier Sci., New York.

Fischer, H. B., J. E. List, C. R. Koh, G. Imberger, and N. H. Brooks (1979), *Mixing in Inland and Coastal Waters*, 483 pp., Academic, New York.

Gourlay, M. R. (1996a), Wave set-up on coral reefs. Part 1. Set-up and wave-generated flow on an idealised two dimensional horizontal reef, *Coastal Eng.*, *27*, 161–193, doi:10.1016/0378-3839(96)00008-7.

Gourlay, M. R. (1996b), Wave set-up on coral reefs. Part 2. Set-up on reefs with various profiles, *Coastal Eng.*, *28*, 17–55, doi:10.1016/0378-3839(96)00009-9.

Gourlay, M. R., and G. Colleter (2005), Wave-generated flow on coral reefs—An analysis for two dimensional horizontal reef-tops with steep faces, *Coastal Eng.*, *52*, 353–387, doi:10.1016/j.coastaleng.2004.11.007.

Grigg, R. W. (1998), Holocene coral reef accretion in Hawaii: A function of wave exposure and sea level history, *Coral Reefs*, *17*, 263–272, doi:10.1007/s003380050127.

Guza, R. T., and E. B. Thornton (1981), Wave set-up on a natural beach, *J. Geophys. Res.*, *86*, 4133–4137, doi:10.1029/JC086iC05p04133.

Hearn, C. J. (1999), Wave-breaking hydrodynamics within coral reef systems and the effect of changing relative sea level, *J. Geophys. Res.*, *104*, 30,007–30,019, doi:10.1029/1999JC900262.

Hearn, C. J., and I. N. Parker (1988), Hydrodynamic processes on the Ningaloo coral reef, paper presented at 6th International Coral Reef Symposium, International Society of Reef Study, Townsville, Queensland, Australia, 8–12 Aug.

Hearn, C. J., B. G. Hatcher, R. J. Masini, and C. J. Simpson (1986), Oceanographic processes on the Ningaloo coral reef, *Environ. Dyn. Rep. ED-86-171*, Dep. of Conservation and Land Manage., Perth, West. Aust., Australia.

Hench, J. L., J. J. Leichter, and S. G. Monismith (2008), Episodic circulation and exchange in a wave-driven coral reef and lagoon system, *Limnol. Oceanogr.*, *53*, 2681–2694, doi:10.4319/lo.2008.53.6.2681.

Kamphuis, J. W. (2000), *Introduction to Coastal Engineering and Management*, 437 pp., World Sci., Singapore.

Kennedy, D. M., and C. D. Woodroffe (2002), Fringing reef growth and morphology: A review, *Earth Sci. Rev.*, *57*, 255–277, doi:10.1016/S0012-8252(01)00077-0.

Kraines, S. B., T. Yanagi, M. Isobe, and H. Komiyama (1998), Wind-wave driven circulation on the coral reef at Bora Bay, Miyako Island, coral reefs, *Coral Reefs*, *17*, 133–143.

Kraines, S. B., A. Suzuki, T. Yanagi, M. Isobe, X. Y. Guo, and H. Komiyama (1999), Rapid water exchange between the lagoon and the open ocean at Majuro Atoll due to wind, waves, and tide, *J. Geophys. Res.*, *104*, 15,635–15,653, doi:10.1029/1999JC900065.

Kraines, S. B., M. Isobe, and H. Komiyama (2001), Seasonal variations in the exchange of water and water-borne particles at Majuro Atoll, the Republic of the Marshall Islands, *Coral Reefs*, *20*, 330–340, doi:10.1007/s00338-001-0191-8.

Large, W. G., and S. Pond (1981), Open ocean momentum flux measurements in moderate to strong winds, *J. Phys. Oceanogr.*, *11*, 324–336.

Longuet-Higgins, M. S., and R. W. Stewart (1964), Radiation stresses in water waves; a physical discussion, with applications, *Deep Sea Res.*, *11*, 529–562.

Lowe, R. J., J. L. Falter, S. G. Monismith, and M. J. Atkinson (2009a), A numerical study of circulation in a coastal reef-lagoon system, *J. Geophys. Res.*, *114*, C06022, doi:10.1029/2008JC005081.

Lowe, R. J., J. L. Falter, S. G. Monismith, and M. J. Atkinson (2009b), Wave-driven circulation of a coastal reef-lagoon system, *J. Phys. Oceanogr.*, *39*, 873–893, doi:10.1175/2008JPO3958.1.

Lugo-Fernández, A., H. H. Roberts, and W. J. Wiseman Jr. (2004), Currents, water levels, and mass transport over a modern Caribbean coral reef: Tague Reef, St. Croix, USVI, *Cont. Shelf Res.*, *24*, 1989–2009, doi:10.1016/j.csr.2004.07.004.

MacMahan, J. H., E. B. Thornton, and A. J. H. M. Reniers (2006), Rip current review, *Coastal Eng.*, *53*, 191–208, doi:10.1016/j.coastaleng.2005.10.009.

Monismith, S. G. (2007), Hydrodynamics of coral reefs, *Annu. Rev. Fluid Mech.*, *39*, 37–55, doi:10.1146/annurev.fluid.38.050304.092125.

Monsen, N. E., J. E. Cloern, L. V. Lucas, and S. G. Monismith (2002), A comment on the use of flushing time, residence time, and age as transport time scales, *Limnol. Oceanogr.*, *47*, 1545–1553, doi:10.4319/lo.2002.47.5.1545.

Pattiaratchi, C. B. (1994), Physical oceanographic aspects of the dispersal of coral spawn slicks: A review, in *The Biophysics of Marine Larval Dispersal, Coastal Estuarine Sci. Ser.*, vol. 45, edited by P. W. Sammarco and M. L. Heron, pp. 89–105, AGU, Washington, D. C.

Pawlowicz, R., B. Beardsley, and S. Lentz (2002), Classical tidal harmonic analysis including error estimates in MATLAB using T-TIDE, *Comput. Geosci.*, *28*, 929–937, doi:10.1016/S0098-3004(02)00013-4.

Symonds, G., K. P. Black, and I. R. Young (1995), Wave-driven flow over shallow reefs, *J. Geophys. Res.*, *100*, 2639–2648, doi:10.1029/94JC02736.

Tartinville, B., E. Deleersnijder, and J. Rancher (1997), The water residence time in the Mururoa atoll lagoon: Sensitivity analysis of a three-dimensional model, *Coral Reefs*, *16*, 193–203, doi:10.1007/s003380050074.

Wiens, H. J. (1962), *Atoll Environment and Ecology*, 532 pp., Yale Univ. Press, New Haven, Conn.

Wyatt, A. S., R. J. Lowe, S. Humphries, and A. M. Waite (2010), Particulate nutrient fluxes over a fringing coral reef: Relevant scales of phytoplankton production and mechanisms of supply, *Mar. Ecol. Prog. Ser.*, *405*, 113–130.

R. Brinkman, Australian Institute of Marine Science, PMB 3, Townsville, Qld 4810, Australia.

G. N. Ivey, C. B. Pattiaratchi, and S. Taebi, School of Environmental Systems Engineering, University of Western Australia, Crawley, WA 6009, Australia.

R. J. Lowe, School of Earth and Environment, University of Western Australia, Crawley, WA 6009, Australia.

G. Symonds, CSIRO Marine and Atmospheric Research, Underwood Avenue, Floreat, WA 6014, Australia.